Proceedings of the Korean Nuclear Society Spring Meeting
Cheju, Korea, May 2001

A Transition Cycle Strategy to Enhance Minor Actinide Burning Potential in the Pan-Shape LMR Core

Sang Ji Kim, Young Il Kim and Young Jin Kim
Korea Atomic Energy Research Institute,
150 Dukjin-dong, Yusong-gu, Taejon, 305-353, Korea

Nam Zin Cho
Korea Advanced Institute of Science and Technology
373-1 Kusong-dong, Yusong-gu, Taejon, 305-701, Korea

Abstract

This study summarizes the neutronic performances and fuel cycle behaviors of the pan-shape transuranic (TRU) burner core from the initial core through the end of a core life. The cycle-by-cycle evolution of isotopic compositions and neutronics characteristics are compared with those calculated from the analysis of an assumed equilibrium cycle. The amount of burnt TRU per cycle after Cycle 8 turned out to be comparable to that of the equilibrium cycle, while the isotopic compositions and the resulting neutronics performances up to about Cycle 20 have shown considerable deviations from those of the equilibrium cycle. The reference core in this analysis has been designed to meet a target sodium void reactivity at the end of the equilibrium cycle by reducing the active core height. Since the core isotopic loading approaches that of the equilibrium cycle after many cycles of operation, significant margins to the target sodium void reactivity are noted in the early cycles. This finding has led to the loading of concentrated minor actinides (MA) relative to the Pu isotopes in the first three cycles. Thereafter, they are homogeneously self-recycled with the external feed TRU makeup composed of typical LWR discharge TRU compositions. The transition cycle analysis with the higher MA loading reveals that the total MA consumed through 50 cycles of operation is 1.89 times larger than the case for the constant external feed makeup TRU with a typical LWR discharge compositions, without exceeding the sodium void reactivity observed in the equilibrium cycle.

1. Introduction

A variety of metallic fueled, TRU burner designs, which can achieve the sodium void reactivity reduction, have been developed in the past. These design studies have investigated the performance trends and void reactivities for design changes such as introducing moderating materials, sodium volume fraction increase, core geometry flattening and annular cores placing large central blanket or central absorber island. In general, the reduction of the sodium void reactivity is in contradiction with a good neutron economy and thus leads to the

deterioration of core neutronic performances.

For the analysts' convenience, a conceptual study on transuranic burner core designs is typically performed with specified TRU compositions for the freshly charged assemblies (namely, once-through equilibrium without recycling) or with the assumption of self-recycling in a given external feed TRU composition (namely, the self-recycled equilibrium). These strategies allow the avoidance of performing the routine and time consuming transition cycle analysis which is continued until the equilibrium cycle is achieved, starting from the initial core. The resulting neutronic and safety characteristics from the equilibrium cycle analysis are believed to be reasonable indicators for the reactor under consideration after many cycles of operation. When the self-recycling of transuranic elements like the case for the transuranic burner cores is subject to the transition cycles, the deterioration of plutonium vector (toward higher weight percent of even numbered Pu) changes core neutronic performance and safety parameters. The adverse effects of degraded Pu quality to the core performance have been investigated with the assumption of the once-through equilibrium cycle [1-3]. With the self-recycling imposed, Ref. 4 is credited to first report the approximate evolution of TRU concentrations during the transition cycles in the open literature.

The focus of this study is given on a realistic transition cycle analysis of a pan-shape TRU burner design [5], which is developed to achieve a negative sodium void reactivity subject to the TRU burner core envelope. The core geometry of the reference pan-shape transuranic burner core was determined to satisfy a given target sodium void reactivity at the end of the equilibrium cycle (EOEC) when the evaluated sodium void reactivity is the least negative. The way of achieving the target sodium void reactivity was to reduce the active core height until the satisfactory results in the sodium void reactivity and maximum peak power density are obtained with the self-recycled equilibrium cycle compositions. Therefore, one would expect that the degree of "pancaking" of the active core could be reduced if the equilibrium cycle is never reached by the end of the expected core life (~50 years). And, if the equilibrium cycle is reached after many cycles, the prior cycles can accommodate a higher MA loading to enhance MA consumption. This study was launched to quantify these possible benefits.

2. Reference Core Description

The reference core for the TRU transmutation is developed in Ref. 5, and it went through the optimization process [6]. The final core layout after the optimization is depicted in Fig. 1. The core power rating is 1575 MWt and uses U-TRU-10Zr metallic fuels. The main mechanism of the design concept to achieve a low sodium void reactivity is via the axial leakage upon the formation of sodium void. This core has maximum "pancaking" in the inner core, while the longer outer core fuels compensate for the small power sharing of shorter inner core fuels. In this manner, the flat power distribution is obtained even with the use of a single enrichment. In addition, the local void reactivity is fairly uniform all over the core, still resulting in a small sodium void reactivity.

There are 192 short fuels and 180 long fuels. The surface to volume ratio of the core is 0.064. The control system consists of 31 control rods and 18 shutdown rods, which provides a negative reactivity well over the reactivity control requirement.

3. Equilibrium Cycle Analysis

The core layout shown in Fig. 1 has been determined through the optimization process in the equilibrium cycle mode of REBUS-3 code [7]. The relevant fuel cycle assumptions for the core neutronic evaluation are

given in Table 1. Since the transition cycle analysis in the following sections assumes that the reprocessing and refabrication occur in the first day of reloading, these time durations in the equilibrium cycle are consistently set to zeroes. The isotopic compositions of LWR discharged TRU in Table 2 are used as external feed Pu and MA compositions throughout this study.

Nuclear performance parameters and TRU mass flow data of the equilibrium cycle are summarized in Table 3. The burnup reactivity swing of 4.71%Δρ incurs a large reactivity hold down requirement at BOEC. The TRU enrichment of charged fuel is 35.9 w/o (31.2 w/o Pu, 4.7 w/o MA). The 83.9% of the charged TRU mass is the self-recycled material. The external feed mass flow rate of LWR TRU nuclides is 298 kg/year. The annual consumption of U-238 is 213 kg, of which 75.6% is transmuted to TRU nuclides. MAs are consumed at a rate of 33 kg/year. A notable composition difference between the external feed TRUs and BOEC inventory is a significant deterioration of the plutonium vector and an increase in the Pu-240 fraction. Cm isotopes other than Cm-245 are being produced in the reactor core. Since Cm-242 and Cm-244 decay with the half-life of 163 days and 17.9 years, respectively during the outage and the discharge cooling time, the EOEC loading is larger than that of BOEC.

The fuel cycle options were studied in the equilibrium cycle to see the impacts of nuclide composition changes to the neutronic performance parameters, motivated by the large difference in the TRU compositions between the external feed and EOEC core compositions. The results are summarized in Table 4. In the once-through equilibrium cycle without TRU recycling, this core consumes only 20 kg/year of MA, and it burns plutonium preferentially at a rate of 258 kg/year. In the initial core, the MA burning rate reduces to 14 kg. When the reactor is assumed to operate for 50 cycles, the MA burning through the core life is approximately estimated to be 1699 kg. The infinitely recycled equilibrium core suffers an increase in TRU charge enrichment (from 30.1 to 35.9 TRU w/o), but exhibits a reduced burnup swing (from 5.87 %Δρ to 4.71 %Δρ). During the development of the pan-shape core of Fig. 1, the critical factor in determining the core geometry was the sodium void reactivity at EOEC when the sodium void reactivity is the least negative. The safety analysis and set point analysis will be based on the neutronic performance data when the lowest possible quality of Pu is loaded. Table 4 suggests that the extreme pancaking of the core can be postponed until the equilibrium cycle concentration is reached. Before the equilibrium cycle is attained, there are huge margins to the sodium void reactivity for which the safety analysis already accounted. One way to make use of this fact is that the TRU burner core can be optimized to improve MA consumption, still satisfying the cycle independent target void reactivity at EOEC. Therefore, the explicit cycle-by-cycle analysis needs to be performed in order to know the cycle number when the equilibrium cycle concentrations are reached. Typically in the reactors with the high breeding ratio, the deterioration of Pu vector is resisted by the production of the high quality Pu generated in the internal and radial blankets. For the TRU burners, the refreshment of Pu is only achieved from the external feed, and the quality of loaded Pu becomes poorer if the recycle fraction is high as is the case for the current design under investigation.

4. Transition Cycles with Constant External Feed TRU Compositions

An explicit fuel loading was exercised by designating the position of each fuel assembly in a specific location for every cycle. The initial core assumed uniform charge enrichment for every assembly. Since the core is to be operated in a three batch reload scheme, the assemblies with the stage number 3 in Fig. 1 were discharged at the end of the initial core, and allowed to cool until the first day of Cycle 4. At the first day of Cycle 4, the

discharged assemblies at the initial core are reprocessed and mixed with the variable amount of LWR discharged external feed TRU's to meet the cycle length of 310 effective full power days (EFPD) of Cycle 4. The external feed TRU fraction to the total heavy metal together with the recycled TRU was varied to result in the core eigenvalue of unity at each end of the given cycle. The cycle length was fixed to 310 EFPD for every cycle. The cycle two and three feed fuels consist of the external feed fuels alone. The explicit fuel cycle analysis has gone to the 80^{th} cycle.

The evolution of each nuclide mass at EOC of every cycle is shown in Figures 2 and 3 for Pu isotopes and MA nuclides, respectively. Between Cycles 82 and 90, the EOEC TRU masses given in Table 3 are plotted. Although 84% of the charged TRU mass is self-recycled, Pu isotopic compositions slowly approach those for the equilibrium cycle loading. Especially, Pu-240 shows a slow transition to that of the equilibrium cycle and the amount of change per cycle is significant. The loaded Pu-240 mass at EOC is less than 90% of the equilibrium cycle EOC loading until the core reaches Cycle 28. In addition, 10% of the Pu-240 mass amounts to as large as 155 kg. Considering that the EOEC core total MA loading is 656 kg, this is a significant amount of mass to alter the core neutronic performance at Cycle 28. Pu-242 needs 51 cycles for the EOC loading to reach 90% of that in the equilibrium cycle.

Each MA nuclide is also approaching the equilibrium cycle concentration. Except Np-237, every other MA concentrations at the initial core are smaller than the equilibrium cycle concentrations. Am-241 approaches rapidly the equilibrium cycle mass and takes 90% of the equilibrium cycle mass at Cycle 6, since the EOC loading of its parent nuclide, Pu-241 falls within 110% of the equilibrium cycle mass in 8 cycles. For the first three cycles, Am-241 is being produced from the relatively large amount of Pu-241. In turn, this implies that the MA burning in the early cycles will be fairly low, compared with the equilibrium cycle when the Am-241 burning comprises about 46% of total MA burnt. Np-237, Am-243, Cm-244 needs 35, 49 and 66 cycles in order for their respective loading to fall within 10% from the respective equilibrium cycle EOC loading. Am-243 burns throughout the reactor lifetime, but the fresh external feed surpasses the burnt amount until the equilibrium cycle for the Am-243 is attained. Cm-242 and Cm-244 are always more produced than consumed in the reactor core because of the neutron captures in Am-241 and Am-243. The equilibrium Cm-244 concentration is achieved by balancing the production in the reactor core plus the external feed and the natural decay into Pu-240. When the 50 cycles of reactor life is assumed, all Cm isotopes except Cm-243 are being produced during the irradiation in the core, especially due to β- decay of Am-242m and Am-244. Concerning with the remaining MA mass at the end of the reactor lifetime, the strategy of irradiation and radioactive decay for Cm isotopes is better than simply separating Cm from other TRU and waiting their decays to Pu isotopes. Other MA in Figure 3 only comprises about 9 w/o of total MA, and the variation is not large enough to alter the core neutronic performance.

It is shown that the addition of MA and even numbered Pu's are the main cause of the less negative sodium void reactivity and less negative fuel temperature coefficient [5]. Moreover, the effect of MA on these two reactivity coefficients is more significant than fertile Pu's. It is expected that the core performance degradation must be retarded over the fairly long early cycles of a reactor lifetime.

The sodium void reactivity and Doppler constant at EOC of each cycle are depicted in Figure 4. The whole core sodium void reactivity becomes monotonically less negative as cycle proceeds. For the first 20 cycles, its gradient is larger. The 50 cycles of operation is required for the sodium void reactivity at EOC to fall within 10% from the equilibrium cycle value. Even at the 40^{th} cycle, the margin to the target EOEC sodium void reactivity is

78 pcm and it is as large as 204 pcm at Cycle 20. Figure 4 also shows that the sodium void reactivity and Doppler constant share remarkably well the same transition cycle behaviors toward their respective equilibrium cycle values. For both reactivity coefficients, the MA contents play the major role to determine them. Overall, the equilibrium cycle analysis tends to unnecessarily jeopardize the core design, remembering that the sodium void reactivity was a critical factor in determining the degree of "pancaking" the core geometry. The target sodium void reactivity based on the equilibrium cycle analysis results in the penalty in the fuel cycle costs due to the extreme core pancaking and its eventual core diameter increase. Alleviation of this would be beneficial with respect to the decrease in the fuel reprocessing burden or nullifying the requirement of other design provisions such as a limited amount of MA loading or spectrum softening material introduction.

5. Transition Cycles with Variable External Feed TRU Compositions

Since the core sodium void reactivity in the transition cycle never reaches that of the equilibrium cycle and there is an appreciable margin to the target sodium void reactivity up to Cycle 20, the enriched minor actinides are decided to be loaded in the first three cycles. The weight fraction of MA among external feed TRU was adjusted to result in the least negative sodium void reactivity over the 50 cycles more negative than that identified at the EOEC. Through the variation study on the external feed TRU compositions for the first three cycles, the finally determined MA w/o among the TRU for the first three cycle feeds is as high as 26 w/o. From the 4^{th} cycle, the external feed TRU compositions return to the typical LWR discharge and thus, consists of 11w/o MA of which compositions are given in Table 2.

The evolution of each nuclide mass at EOC of every cycle is shown in Figures 5 and 6 for Pu isotopes and MA nuclides, respectively. Between Cycles 82 and 90, the EOEC TRU masses given in Table 3 are plotted. Because the discharges of first three cycles with high contents of MA are recycled into Cycle 4 and later cycles, the cycles following Cycle 3 also have high fractions of MA among TRU nuclides. The mass evolution of Pu isotopic compositions is essentially indifferent from the case with the constant external feed TRU compositions. This provides the opportunity for the increased MA loading in the early cycles before the Pu vector is deteriorated. If Pu-240 accumulates rapidly toward the equilibrium cycle concentration, there will be little possibility of embedding a higher MA concentration. Pu-240 loading falls within 90% of the EOEC loading at Cycle 34, and Pu242 needs 57 cycles. Due to the smaller amount of Pu loading at the first three cycles, the time when the loading of even numbered Pu takes 90% of the equilibrium cycle value, is postponed by six or seven cycles.

Each MA is also approaching the equilibrium cycle concentrations. Except Np-237, Am-241 and Am-243, every other MA concentrations at the initial core are smaller than the equilibrium cycle concentrations. Because these three MA can be burnt in the core, the burning amounts of these nuclides in the early cycles are very high. For example, at the initial core Np-237, Am-241 and Am-243 burns by 67.6 kg, 21.1 kg, and 28.3 kg, respectively. The overall MA burning at the initial core is diminished by the net production of Cm-242 and Cm-244 by 11.2 and 17.5 kg, respectively. Am-241 loading takes 90% of the equilibrium cycle mass at Cycle 24. Am-241 is being burnt for every cycle, while Am-241 in the first three cycles for the constant external feed TRU case is being produced from the relatively large amount of Pu-241. This implies that the MA burning in the early cycles will be fairly large. Np-237, Am-241, Am-243 and Cm-244 need 50, 24, 21 and 7 cycles, respectively in order for their respective loading to fall within 10% from the respective equilibrium cycle EOC loading. Am-243

burns throughout the reactor lifetime, but the burning rate reduces from 28.3 kg at the initial core to 7.2 kg at Cycle 50. More Cm-244 is always produced rather than consumed in the reactor core.

Figure 7 shows the cycle-by-cycle reactivity coefficients when the variable MA content in external feed TRU are used. The least negative sodium void reactivity is –0.53%Δρ, which just misses the EOEC target sodium void reactivity of –0.54%Δρ. This occurs in Cycle 13. The least negative DC of -1.64×10^{-3} is observed in Cycle 3, and it is less negative by 0.24×10^{-3} than that of the EOEC. The saw-tooth shape seen in the sodium void reactivity reflects 3 batch reloads. This is not seen after 20th cycles simply because the reactivity coefficient calculations are performed in every 5 cycle after the 20th cycle. The small negative DC is characteristic of metallic fueled TRU burners without the blanket assemblies. These small temperature coefficients would have to be compensated for by the large axial thermal expansion effect.

By allowing the loading of concentrated MA in the first three cycles, the average MA loading over the expected 50 years of operation is increased, without exceeding the target sodium void reactivity. The increased MA loading is translated into the increased MA transmutation. Table 5 compares the cumulative external feed and the consumed TRU's throughout the 50 year reactor life time for the constant and variable external feed TRU cases. The difference between the feed and the consumed is what remains in the reactor core of 50th cycle EOC and two previous discharges being cooled in the spent fuel storage pool. The negative sign means there is a net production. Np-237 and Am-243 burn out steadily throughout the reactor lifetime, and thus show high consumption fractions of 80% and 58% even for the constant external feed TRU case. These fractions go up to 86% and 72% for the variable external feed TRU case. Like Cm isotopes, Am-242m is also being produced in every cycle. This table reveals that the variable loading has allowed an 89% larger amount of MA burning over its expected 50 cycles of operation, compared with the case of a constant external feed composition. In contrast, the Pu burning is reduced by 7%. At the end of Cycle 50, the remaining TRU nuclide masses are almost identical in both cases.

The total consumption of MA over 50 cycles from the equilibrium cycle analysis is projected to be 1699 kg, based on Table 3. Namely, it is over-predicted by 19% than the MA consumption by the transition cycle analysis. The preferential MA burning is strongly desired when the Pu is viewed as a valuable resource for the future electricity generation or for use in PWR's as mixed oxide fuels. A main cause of large differences in MA burning between two different transition cycles is attributed to the high transmutation rate of Pu into MA due to relatively high concentrations of Pu to MA. For the constant external feed, the total minor actinide burning rates reach the 90% of the equilibrium cycle values after 9 cycles. For the variable external feed TRU, it reaches the 110% of the equilibrium cycle burning rate after 42 cycles of operation. Because the cycle length and core power are fixed, the total heavy metal burning rate is indifferent between the transition cycle and the equilibrium cycle. In order to maximize the MA burning throughout the core lifetime, it is important to keep the loaded MA in any cycle higher than that in the equilibrium cycle.

6. Conclusions

The conclusions drawn from the comparisons between the transition cycle analysis and the equilibrium cycle analysis are as follows:

1. LWR discharged plutonium vector tends to deteriorate up to the 30th cycle and afterwards approaches slowly to the isotopic compositions of the equilibrium cycle. Even in the EOC of the 50th cycle, the EOC plutonium

isotopic compositions deviate from those of the equilibrium cycle. The concentrations of Pu-238, Pu-240 and Pu-242 are still rising.

2. Total minor actinide burning rates reach the equilibrium cycle values just after 9 cycles. Because the cycle length and core power are fixed, the total transuranic burning rate is indifferent between the transition cycle and the equilibrium cycle.
3. Individual minor actinide concentrations do not reach those of the equilibrium cycle even after 50 cycles. Especially, the concentrations of Am-243 and Cm-244 are still rising rapidly.
4. Overall, minor actinide burning is overestimated in the equilibrium cycle analysis by 19%, compared with that of transition cycle analysis.
5. The whole core sodium void reactivity becomes monotonically less negative as cycle proceeds. For the first 20 cycles, its gradient is larger. Even at the 50^{th} cycle, the EOC sodium void reactivity is more negative that that of the equilibrium cycle by 52 pcm.
6. It is perceived that the safety analysis should be done when the Pu quality is the lowest. However, the nuclear design should also focus on the early cycles of the TRU burners in order to enhance the TRU transmutation capability.

The transition cycle analysis has opened new avenues for the further optimization, which is not seen in the conventional equilibrium cycle analysis. As an outcome of this study, the enriched MA loading at the first three cycles results in the following merits and demerits:

7. The enriched MA relative to the Pu can be loaded in the early cycles before the Pu quality is degraded, still preserving the target sodium void reactivity determined at EOEC.
8. By this manner, the MA burning over 50 cycles of operation can be 1.89 times more.
9. The Doppler constants are less negative than that at EOEC.

Acknowledgements

This work was supported by Nuclear R&D Long-Term Development Program of the Ministry of Science and Technology of Korea.

References

1. T. Wakabayashi, K. Takahashi, “Feasibility Studies on Plutonium and Minor Actinide Burning in Fast Reactors,” *Nucl. Technol*., 118, 14 (1997).
2. J. Rouault, J. C. Garnier, A. Languille, “The Design of U Free Large Fast Reactor Cores,” Proceedings, *Proc. Int. Conf. Physics of Reactors*, Mito, Japan, September 16-20, 1996, Vol. 3, p. H.11, Atomic Energy Society of Japan (1996).
3. S. N. Hunter, “Pu Vector Sensitivity for a 600 MW(e) Pu Burning, Fast Reactor,” *Proc. Int. Conf. Physics of Reactors*, Mito, Japan, September 16-20, 1996, Vol. 3, p. H1, Atomic Energy Society of Japan (1996).
4. J. Journet, et al, “Minor Actinide Transmutation in Oxide Fuelled Fast Reactors,” Proc. Int. Conf. Future Nuclear Systems, Seattle, U.S.A., September 12-17, 1993, Vol. 1, p. 99, American Nuclear Society (1993).
5. S. J. Kim, N. Z. Cho, Y. J. Kim, “A Pan-Shape Transuranic Burner Core with a Low Sodium Void Worth,” Ann. of Nucl. Energy, 27, 435 (2000).

6. S. J. Kim, N. Z. Cho, Y. J. Kim, "A Comparative Design Analysis of Transuranic Burner Cores with Low Sodium Void Worths," *Proc. Int. Topl. Mtg. Advances in Reactor Physics and Mathematics and Computation into the Next Millennium*, Pittsburgh, U.S.A., May 7-12, 2000, American Nuclear Society (2000).
7. B. J. Toppel, "The Fuel Cycle Analysis Capability REBUS-3," ANL-83-2, ANL (1983).

Table 1. Fuel cycle assumptions

Reactor Power (MWt)	1575
Cycle Length (days)	365
Capacity Factor (%)	85
Core Driver Refueling per Cycle	1/3
Cooling Time (year)	
LWR Discharge	3.17
TRU Burner Discharge	2.15
Reprocessing Time (month)	0
Refabrication Time (month)	0
TRU Recovery Factor	1.00

Table 2. LWR transuranic isotopes after 3.17 year cooling

Isotope	Wt fraction	Isotope	Wt fraction
Pu-238	1.01E-02	Np-237	5.40E-02
Pu-239	0.508	Am-241	2.51E-02
Pu-240	0.199	Am-242m	1.11E-04
Pu-241	0.134	Am-243	2.48E-02
Pu-242	3.88E-02	Cm-242	9.73E-06
		Cm-243	7.86E-05
		Cm-244	5.52E-03
		Cm-245	5.08E-04
		Cm-246	6.31E-05

Table 3. Equilibrium cycle performance parameters and mass flow

Burnup Swing (%Δρ)	4.71
TRU Conversion Ratio	0.36
Average Discharge Burnup (MWD/kg)	93.41
Peak Local Discharge Burnup(MWD/kg)	123.50
Peak Linear Power (W/cm)	
BOEC	458
EOEC	454
Power Peaking Factor	
BOEC	1.33
EOEC	1.32
Peak Neutron Flux (x 10^{15} n/ cm^2.sec)	
BOEC	4.28
EOEC	4.55
Peak Fast Fluence (x 10^{23} n/cm^2)	2.65
Charge Fuel TRU Enrichment (w/o)	35.94

Mass Flows for Infinite Recycle (kg)

Isotope	BOEC	EOEC	Diff.	Ext. Feed
U-238	9639.5	9426.7	-212.8	
Np-237	151.3	135.2	-16.1	15.9
Pu-238	203.8	198.8	-4.9	3.0
Pu-239	1919.4	1768.3	-151.0	151.0
Pu-240	1612.5	1549.9	-62.6	59.4
Pu-241	326.2	294.5	-31.6	40.2
Pu-242	471.5	459.8	-11.7	11.7
Am-241	193.5	177.6	-15.9	7.5
Am-242m	16.8	16.9	0.0	0.0
Am-243	166.2	158.7	-7.5	7.5
Cm-242	6.4	9.4	3.1	0.0
Cm-243	0.9	0.8	0.0	0.0
Cm-244	125.1	126.8	1.7	1.7
Cm-245	21.6	21.4	-0.2	0.2
Cm-246	9.2	9.2	0.0	0.0
TRU	5224.2	4927.4	-296.8	298.2
MA	691.0	656.0	-34.9	32.9

Table 4. Fuel cycle option study

	Infinite Recycle	Once Through	Initial Core
Burnup Swing (%Δρ)	4.71	5.87	5.88
Charge Fuel TRU w/o	35.94	30.10	27.02
TRU Conversion Ratio	0.36	0.39	0.42
EOEC MA Content (w/o)	4.56	3.29	2.98
EOC $Pu_{fissile}$ Fraction	48.30	66.97	69.48
Pu, MA Burn (kg/cycle)	262,35	258,20	246,14
EOC Sodium Void Reac. (%Δρ)	-0.54	-1.26	-1.40

Table 5. Cumulative external feed and consumed TRU by 50 cycles of operation (kg)

	Constant External Feed		Variable External Feed	
Nuclide	Ext. Feed	Consumed	Ext. Feed	Consumed
Np-237	1197.4	959.1	1827.0	1576.1
Pu-238	224.9	-120.4	214.0	-160.8
Pu-239	11359.5	8324.2	10808.4	7788.0
Pu-240	4468.5	1951.1	4251.8	1771.3
Pu-241	3022.5	2544.3	2875.8	2404.6
Pu-242	878.5	192.8	835.9	166.3
Am-241	566.0	257.3	863.6	559.0
Am-242m	2.5	-25.9	3.8	-24.4
Am-243	563.9	324.6	860.3	618.2
Cm-242	0.2	-10.9	0.3	-10.6
Cm-243	1.8	0.5	2.7	1.4
Cm-244	126.0	-51.0	192.3	1.6
Cm-245	11.6	-17.3	17.8	-15.4
Cm-246	1.5	-5.9	2.2	-8.2
Total Pu	19954	12892	18986	11969
Total MA	2471	1431	3770	2698

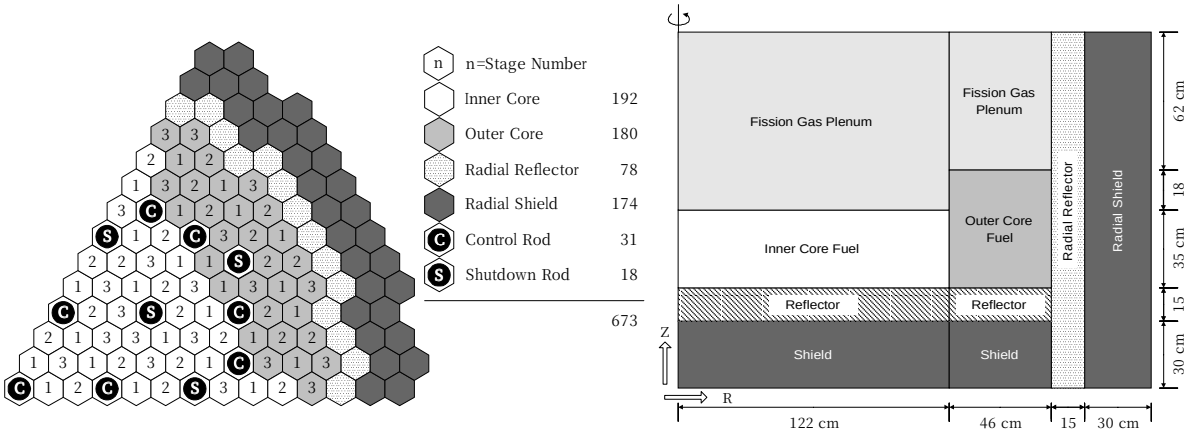

Figure 1. Pan-shape core layout

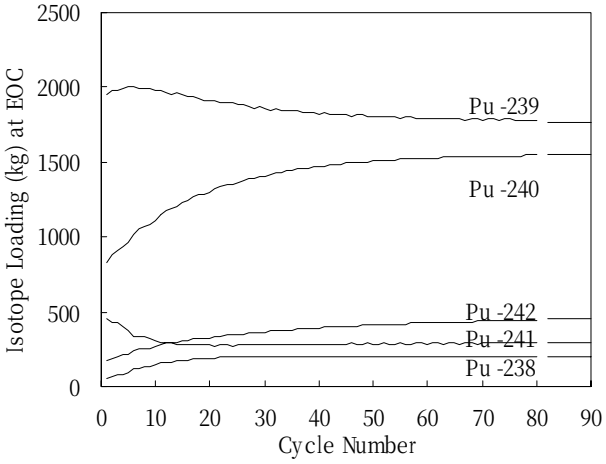

Figure 2. Cyclewise mass of EOC Pu for a constant external feed TRU composition

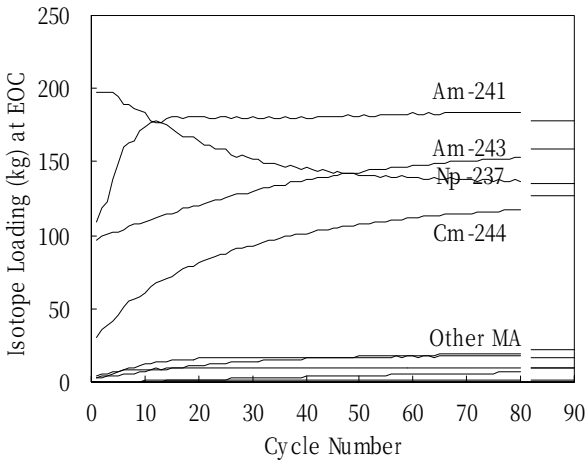

Figure 3. Cyclewise mass of EOC MA for a constant external feed TRU composition

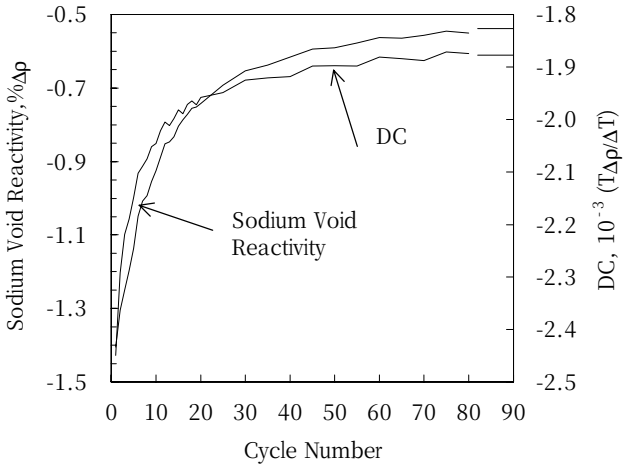

Figure 4. Cyclewise reactivity coefficient for a constant external feed TRU composition

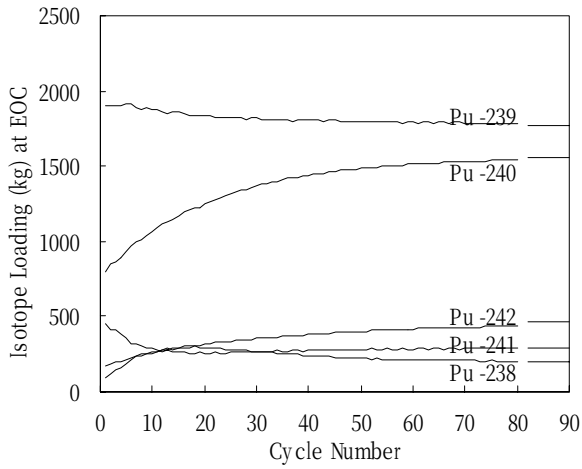

Figure 5. Cyclewise mass of EOC Pu for a variable external feed TRU composition

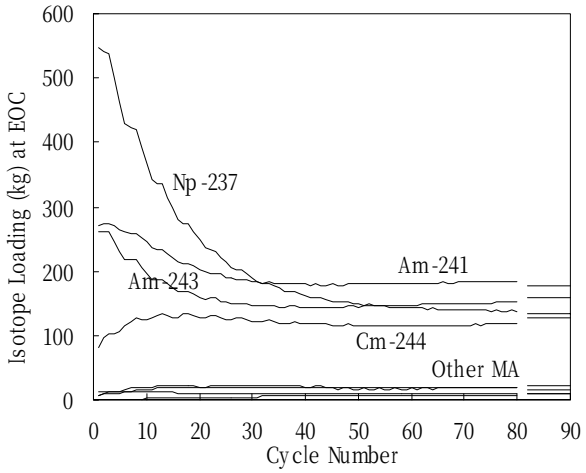

Figure 6. Cyclewise mass of EOC MA for a variable external feed TRU composition

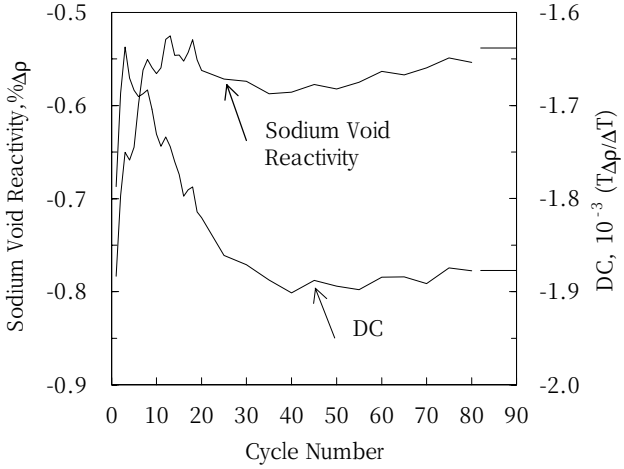

Figure 7. Cyclewise reactivity coefficient for a variable external feed TRU composition